Multiple Steering Molecular Dynamics Applied to Water Exchange at Alkali Ions

Michele Cascella,[†] Leonardo Guidoni,[‡] Amos Maritan,[†,§] Ursula Rothlisberger,[‡] and Paolo Carloni*[,†]

International School of Advanced Studies (SISSA/ISAS) and Istituto Nazionale di Fisica della Materia, Via Beirut 2-4, 34014 Trieste, Italy, Department of Chemistry, ETH Zurich, CH-8093 Zurich, Switzerland, and International Center for Theoretical Physics, 34014 Trieste, Italy

Received: May 30, 2002; In Final Form: October 9, 2002

The novel fast-growth or multiple steering molecular dynamics (MSMD) technique has been recently developed by Jarzynski to calculate free energy profiles along general transformation pathways (*Phys. Rev. Lett.* **1997**, *78*, 2690−2693; *Phys. Rev. E* **1997**, *56*, 5018−5035).[1,2] Here, we apply this approach to calculate free energy barriers involved in the water exchange reaction of Na^+ and K^+ in aqueous solution. We investigate the influence of the key parameters of the MSMD simulations—the steering velocity, the sampling of the initial configurations, and the force constant—on the free energy. Furthermore, we use this approach to describe energetical and structural features of the water exchange reaction of Na^+ and K^+ in aqueous solution. The MSMD technique turns out to be an efficient and fast convergent tool to enhance the sampling of rare chemical events with the help of nonequilibrium forces.

1. Introduction

Hydration and dehydration processes of Na^+ and K^+ ions in aqueous solution play a fundamental role in many biological processes. In ion channels[3] such as the KcsA potassium channel, for instance, the selectivity for potassium over sodium ions is thought to be determined through a ligand exchange reaction that involves the replacement of water molecules with peptidic carbonyl groups.[4,5]

Here, we investigate the water exchange reaction of alkali ions:

$$M(H_2O)_x^+ + H_2O^* \rightleftharpoons M(H_2O^*)(H_2O)_{x-1}^+ + H_2O \quad (1)$$

where M = Na^+ and K^+, and x is a typical coordination number.[6] Our computational approach is the novel multiple steering (or fast growth) molecular dynamics (MSMD) approach proposed by Jarzynski.[1,2,7,8]

MSMD is similar in spirit to the well-known steering dynamics (SD) technique, which has been widely used to provide insight in ligand−receptor binding and in the mechanical unfolding of proteins.[9,10] However, in contrast to SD, MSMD establishes a relation between the nonequilibrium dynamics of the system and its equilibrium properties. It allows us to determine the activation free energy (ΔG) of a given process from a statistical sampling of the irreversible work (W) associated with external, nonconservative forces along a selected reaction coordinate: $\langle e^{-\beta W}\rangle = e^{-\beta \Delta G}$.

This powerful approach has already been applied in a variety of problems. It has been used in the context of single molecule pulling experiments,[11−23] for the calculation of the excess chemical potential of a Lennard-Jones fluid,[24] for the determination of the potential of mean force between two methane molecules in water[25] and for investigating glycerol diffusion in aquaglyceroporins.[26]

In the work presented here the MSMD technique is applied in the context of a ligand substitution reaction. We find that the MSMD methodology enables efficient and accurate calculations of activation barriers and constitutes a promising new tool for the investigation of a wide range of chemical processes.

2. Theory

The MSMD method is described in detail in refs 1, 2, 7, and 8 and will only be briefly summarized here.

The Hamiltonian of a system in the presence of a time-dependent perturbation $u(z,t)$ along a generic reaction coordinate z can be written as

$$H(x,t) = H_0(x) + u(z(x),t) \quad (2)$$

where $H_0(x)$ is a time-independent Hamiltonian and x represents all the coordinates of the system.

We assume that the perturbation term is a harmonic, time-dependent potential along z:

$$u(z,t) = \frac{k}{2}(z - z^0(t))^2 \quad (3)$$

with

$$z^0(t) = z^0(0) + vt \quad (4)$$

where $z^0(0)$ and $z^0(t)$ are the initial and current positions of the minimum of the restraining potential, respectively; v is the steering velocity applied to the system, and $z(t)$ is the position of the system along the coordinate at time t.

The free energy profile along z reads

$$G_0(z) = -\beta^{-1} \ln \frac{\int \delta[z - z(x)] e^{-\beta H_0(x)}\, dx}{\int e^{-\beta H(x,0)}\, dx} \quad (5)$$

* To whom correspondence should be addressed. E-mail: carloni@sissa.it. Telephone: +39-040-3787-405. Fax: +39-040-3787-528.

† International School of Advanced Studies (SISSA/ISAS) and Istituto Nazionale di Fisica della Materia.

‡ ETH Zurich.

§ International Center for Theoretical Physics.

10.1021/jp026209b CCC: $22.00
Published on Web 11/22/2002

which, according to Jarzynski's identity, can be transformed into[8]

$$G_0(z) = -\beta^{-1} \ln\langle \delta(z - z(t)) e^{-\beta[\int_c F(z,t)dz - u(z^0,0)]} \rangle \qquad (6)$$

where $F(z,t)$ is a harmonic force associated with the perturbation potential:

$$F(z,t) = -k(z(t) - z^0(0) - v(t)) \qquad (7)$$

the integral of the force F is calculated along the path from $z(0)$ to $z(t)$ and the brackets indicate an ensemble average over different trajectories starting at positions sampled from the initial equilibrium distribution.

In practical calculations, the average in eq 6 is calculated with a limited set of simulations and the integral to evaluate the work is determined as a time average over each of the finite length trajectories. This unavoidable truncation introduces errors that can be minimized through an optimal choice of three key parameters, namely (i) the steering velocity v in eq 4, (ii) the initial conditions for each simulation, and (iii) the force constant k. The first influences directly the degree of irreversibility of the transformation; the second enters the ensemble average in eq 6 and affects the weight of each simulation; in fact, the initial bias on the steered system enters explicitly in the exponential of the right-hand side of eq 6; the third affects the dynamics of the systems and enters directly in the formulas as well. In the $v \rightarrow 0$ limit the transformation becomes reversible, the distribution of the argument of the exponential in eq 6 becomes infinitly sharp, and we recover the well-known result that the free energy profile $G_0(z)$ coincides with the reversible work done to bring the system from the initial equilibrium state to the final one. We have checked that indeed this is the case for the systems described in the next sections. Moreover, the choice of initial configurations for the multiple MD runs has a direct influence on the efficiency with which the available phase space can be sampled within a limited number of simulations. In particular, it is crucial that the averaging is performed with individual runs that are largely independent and thus uncorrelated. Thus, it may have a crucial influence on the convergence properties. Finally, the choice of the force constant k could influence the convergence of the free energy profile. The convergence behavior with respect to these parameters is tested in this work (see Results).

3. Methods

All the simulations were performed using the AMBER 5 program[27] with the Åqvist,[28] Smith,[29] and TIP3P[30] force fields for Na^+ and K^+ cations, the Cl^- anion, and water, respectively. In each simulation, one alkali ion (either K^+ or Na^+) was immersed in a $20.4 \times 20.4 \times 36.5$ Å^3 tetragonal box containing 421 water molecules and a Cl^- counterion. The latter, which was initially located 15.0 Å far from the alkali ions, remained always farther than 9.0 Å from the cations during the MD simulations. Periodic boundary conditions were applied. Long-range electrostatic interactions were treated via a particle-mesh Ewald procedure[31,32] using a grid of $20 \times 20 \times 36$ points with a cubic spline interpolation. A cutoff of 10.0 Å for the short-range electrostatic, and van der Waals interactions was used. Constant temperature (300 K) and constant pressure (1.0 atm) conditions were achieved by coupling the systems to a Berendsen thermostat and barostat.[33] The integration time step of our simulation was set to 1.5 fs.

All the systems underwent first 0.3 ns of unconstrained MD. Subsequently, the position of one water molecule was restrained using a harmonic potential at a distance of 7.0 Å from the metal ion for 0.24 ns. The structural properties (such as the $g_{HO}(r)$ and $g_{OO}(r)$ radial distribution functions) resemble those of bulk water. A total of 10 snapshots of this MD simulations, taken every 12 ps of dynamics, constituted our initial structures for the MSMD simulations.

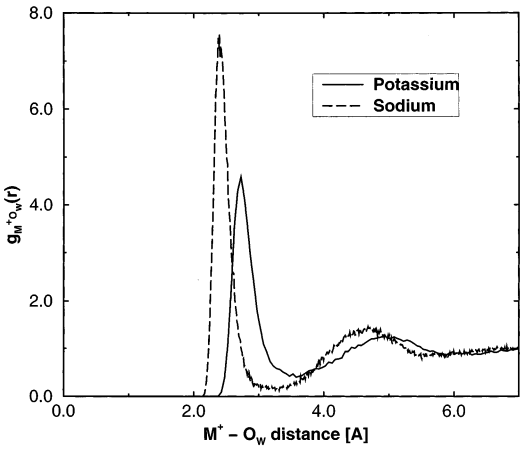

Figure 1. Calculated ion/water radial pair distribution functions ($g_{MO_w}(r)$) for Na^+ and K^+ in aqueous solution.

In the MSMD simulations, the irreversible work W (eq 6) was calculated as the work required to bring the system from the initial equilibrium state (i.e., the left-hand side of eq 1) to its final state (i.e., the right-hand side of eq 1). In practice, the approaching water (WAT hereafter) was steered from the bulk toward the alkali ion (M^+) by applying the time-dependent potential $u(z,t)$ in eq 3. Consistent with the initial conditions, the starting position of the minimum of the harmonic potential $z^0(0)$ (eq 4) was set to 7.0 Å. The calculations were performed until the minimum of the harmonic potential reached a distance of 2.0 Å from the cation. MSMD runs with varying pulling velocities and different choices of the initial MD configurations were performed:

(i) 4 sets of 10 runs with different steering velocities on K^+ ($v = 0.0333$, 0.0667, 0.3333, 0.6666 Å ps^{-1}), each of them with initial configurations sampled every 12 ps and with a force constant $k = 300$ pN Å^{-1};

(ii) 3 sets of 10 runs with different sampling on the starting positions on K^+ (snapshots taken every $\Delta t = 12$, 1.5, 0.15 ps) with a steering velocity $v = 0.0666$ Å ps^{-1} and a force constant $k = 300$ pN Å^{-1};

(iii) 6 sets of 10 runs with different force constants on K^+ ($k = 30$, 60, 100, 500, 1000, 1500 pN Å^{-1}) with $v = 0.0666$ Å ps^{-1} and initial configurations sampled every 12 ps;

(iv) 1 set of 10 runs on Na^+ with $v = 0.0333$ Å ps^{-1} and $k = 300$ pN Å^{-1} and with initial configurations sampled every $\Delta t = 12$ ps.

Coordination numbers of the alkali ions were calculated as integrals of the oxygen (water)−ion radial pair distribution functions (rdf) $g_{MO_w}(r)$ (Figure 1) from $r = 0$ to the first minimum of rdf ($r = 2.7$ and 2.4 Å for potassium and sodium, respectively (Figure 1, Table 1)). Identical integration boundaries were chosen to obtain the corresponding values in the MSMD runs.

4. Results and Discussion

In this section, we first assess the accuracy of our computational scheme. Subsequently, we analyze the structural and energetic properties of sodium and potassium ions in aqueous solution.

TABLE 1: Selected Equilibrium Properties of K^+ and Na^+ in Aqueous Solution

ion	first max.[a]	first min[b]	n[c]	first max. (lit.)[d]	first min. (lit.)[e]	n (lit.)[f]
K^+	2.70	3.65	6.9 (5−10)	2.7−2.9	3.6−3.8	6.3−7.6−8.0
Na^+	2.40	3.25	5.8 (4−7)	2.4	3.2−3.5	4.9−6.0−6.6

[a] First maximum and [b]first minimum of $g_{MO_w}(r)$ (Å) between the ion and water's oxygens and [c]correspondent coordination numbers. The range of coordination numbers is indicated in brackets. [d −f]Properties obtained in previous simulations.[35−39]

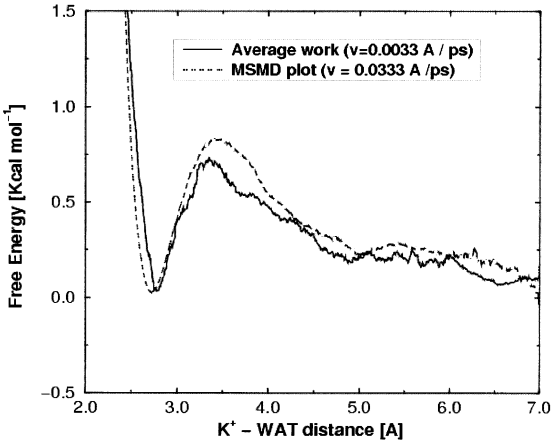

Figure 2. Average work of the transformation at very slow pulling speed ($v = 0.00333$ Å ps^{-1}). This profile is used as a benchmark for the free energy reconstruction profiles obtained at higher pulling speeds.

Accuracy of the Approach. The accuracy of our computational approach was tested through a series of calculations for the water exchange reaction at K^+, for which a classical force field description is known to perform especially well.[34]

In particular, we investigated the dependence of the calculated free energy from (i) the *steering velocities* v in eq 6, (ii) the choice of the *initial configurations*, and (iii) the *force constant* k.

(i) Dependence on v. In this and in the subsequent simulations the initial structures were taken by selecting snapshots from our restrained MD simulation at a time interval of $\Delta t = 12$ ps after the system was equilibrated.

The first reference simulation consists of using an extremely low steering velocity ($v = 0.00333$ Å ps^{-1}) and computing the average work done in moving a water molecule from the bulk to the metal ion. Under this condition, the transformation can be considered quasi-static. Thus, it provides an approximate, reference free energy profile of the process (Figure 2).

If v is one order of magnitude larger ($v = 0.0333$ Å ps^{-1}), the reconstructed MSMD free energy profile turns out to converge within very few simulations (Figure 3a). Indeed, the profile can be considered fully converged after an averaging of ca. 8 trajectories (Figure 3a) and matches well our reference (Figure 2).

In this regime, the free energy profile is qualitatively well described by a single integration of the force along the reaction coordinate (Figure 4a). This indicates that the performed work is essentially conservative and already a single simulation appears to contain sufficient information about the equilibrium properties.

By doubling the steering velocity, convergence to the same value of the free energy barrier is achieved (Table 2, Figure 5). In both this and the previous case, hysteresis effects are essentially absent.

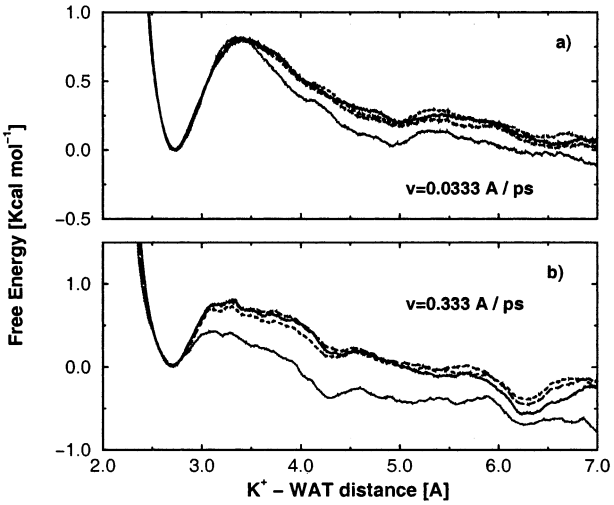

Figure 3. Dependence of the reconstructed free energy of K^+ water exchange reaction on the steering velocity v: (a) $v = 0.0333$ Å ps^{-1}; (b) $v = 0.3333$ Å ps^{-1}. The free energy is obtained averaging data from four (dotted line), six (dashed line), eight (long-dashed), and ten (solid line) MD simulations.

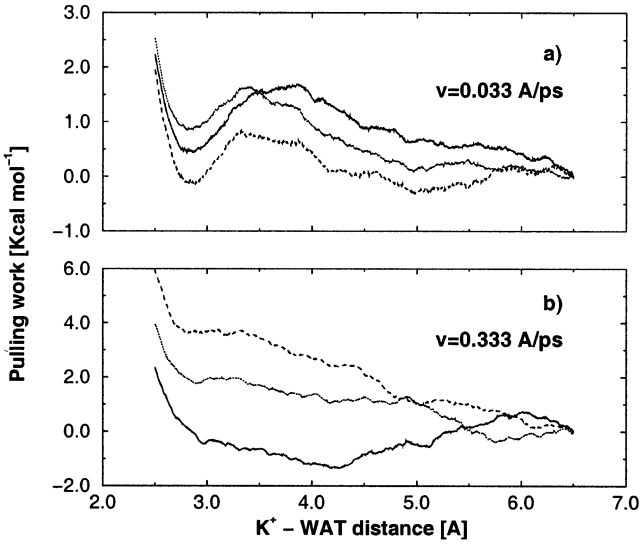

Figure 4. Work associated with single steering dynamics runs at different conditions (see Table 2): (a) $v = 0.0333$ Å ps^{-1}; (b) $v = 0.3333$ Å ps^{-1}.

TABLE 2: Multiple Steering Molecular Dynamics of K^+ and Na^+

ion	v (Å ps^{-1})[a]	$\Delta G^{\ddagger}$ (kcal mol^{-1})[b]	R_0 (Å)[c]	R_{TS} (Å)[d]
K^+	0.0333	0.81	2.72	3.4
K^+	0.0667	0.80	2.73	3.4
K^+	0.3333	0.83	2.70	3.2
K^+	0.6667	0.92	2.70	3.3
Na^+	0.0333	1.30	2.43	3.1

[a] Steering velocity. [b] Calculated activation free energy. [c] M^+−WAT distance corresponding to the minimum of the free energy plot. [d] Distance of M^+−WAT at the TS.

For relatively large velocities ($v = 0.3333$ Å ps^{-1}), the free energy profile does not converge in the bulk region (that is between 7.0 Å and ≈5.5 Å) whereas it is similar to the previous ones in the well region (between ≈3.5 and 2.0 Å) (Figure 3b). In this case, significant hysteresis effects are present, suggesting that the dominant part of the work associated with the steering force is nonconservative (Figure 4b).

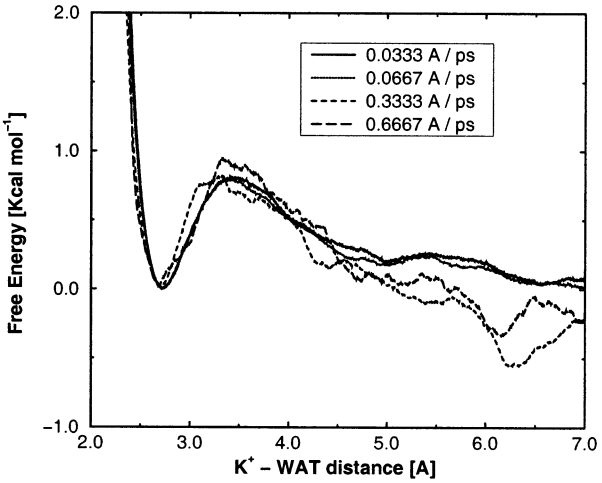

Figure 5. Free energy profile reconstruction for K^+ by using different pulling speeds. The free energy reconstruction profiles obtained at different v for the potassium ion are displayed: $v = 0.0333$ Å ps^{-1} (solid line), $v = 0.0667$ Å ps^{-1} (dotted line), $v = 0.3333$ Å ps^{-1} (dashed line), and $v = 0.6667$ Å ps^{-1} (long-dashed line).

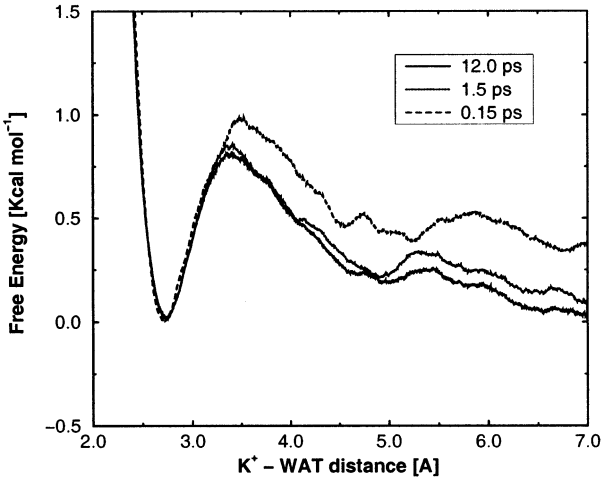

Figure 6. Influence of the initial bias. The three profiles have been calculated by averaging 10 simulations. Each initial condition has been chosen by sampling a biased dynamics run every 12 ps (solid line), 1.5 ps (dotted line), or 0.15 ps (dashed line).

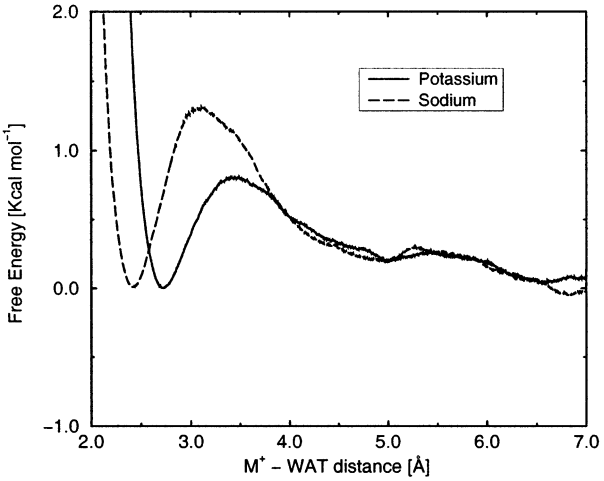

Figure 7. Free energy plots for the two ions. The free energy plots for Na^+ and K^+ are shown. Ten simulations were averaged setting the pulling speed to $v = 0.0333$ Å ps^{-1}, and obtaining the inital conditions sampling every 12 ps a former biased MD simulation.

Upon further increasing the steering velocity ($v = 0.6667$ Å ps^{-1}), the free energy plot in the repulsive region (from ≈5.0 Å to ≈3.5 Å) and in the well region, although rather noisy, is still qualitatively similar to those obtained by pulling at a lower speed (Figure 5). This calculation therefore provides an upper limit for $v \approx 0.05$ Å ps^{-1}.

The qualitative shape of the free energy profile can be understood as follows: when the tagged water molecule is at a large distance from the ion, it is surrounded by an average number of solvating water molecules as given in Table 1. The same situation is also expected when the tagged water molecule is at a particular distance from the ion, substituting, on average, one water molecule from the hydration shell.

We thus expect that the free energy profile shows two minima whose values are the same, one at infinite distance from the ion and the other at a distance typical of the first coordination shell. As the tagged molecule approaches the ion, a divergent profile due to van der Waals repulsion is expected.

(ii) Influence of the Initial Configurations. Varying initial configurations were obtained by selecting snapshots from our restrained MD simulations at different time intervals (Δt). Specifically, three sets of 10 snapshots were considered. In the first $\Delta t = 12$ ps, in the second $\Delta t = 1.5$ ps, and in the third $\Delta t = 0.15$ ps (see Methods). The same steering velocity ($v = 0.0666$ Å ps^{-1}) was used for all calculations.

The reconstructed free energy profiles of the first two sets are rather similar and well converged (Figure 6). In contrast, the free energy profile in the third set does not converge within the 10 simulations carried out here. This suggests that the initial configurations are not independent enough, resulting in an insufficient sampling of phase space.

(iii) Choice of the Force Constant k. Calculations with values of k around the recently reported value of ref 26 (from 30 to 1500 pN Å^{-1}) were performed. It is found that from $k > 60$ pN Å^{-1} up to $k < 1000$ pN Å^{-1} the convergence is fast and no significant changes are found in the profiles.

In conclusion, our analysis allows us to establish the following criteria for the choice of the three computational key parameters: (i) the steering velocity is $v \leq 0.05$ Å ps^{-1}; (ii) initial configurations were sampled at a time interval of $\Delta t \geq 1.5$ ps; (iii) the force constant should be of the order of ≈100−600 pN Å^{-1}. Within these conditions, the convergence on the free energy appears to be rather fast. It should be noted, however, that for more extended systems than those used here, Hummer's cumulant expansion approaches might be required to improve the convergence.[25]

For all simulations of reaction 1, we used $v = 0.0333$ Å ps^{-1}, $\Delta t = 12$ ps, and $k = 300$ pN Å^{-1}. These values compare well with those used in the MSMD simulations of aquaglyceroporin of ref 26. The free energy profiles obtained by using these parameters for both of the two cations are shown in Figure 7.

Potassium. In the unconstrained simulation of a potassium ion in aqueous solution, the metal ion exhibits a labile coordination sphere (average coordination number 6.9). Seven water molecules coordinate K^+ for about half of the simulated time (0.15 ns). The $n = 8$ coordination is also significant (about 28% of the time). In the rest of the dynamics, K^+ is coordinated to a largely varying number of ligands (Table 1). The observed coordination numbers and their average is in good agreement with other data present in the literature[35−39] and with the one of ab initio MD simulations.[34]

The exchange reaction 1 occurs spontaneously during the dynamics. The overall process takes place within as short a time as 0.5 ps in qualitative agreement with previous findings.[34−38]

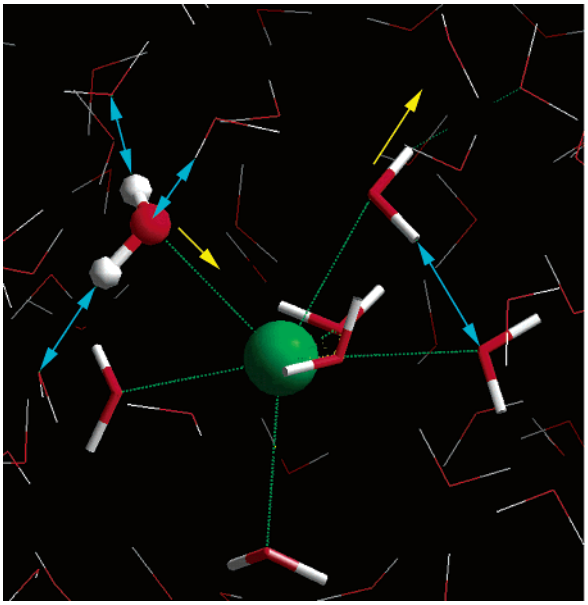

Figure 8. Transition state geometry of reaction 1 for the potassium ion. The incoming water (WAT) is represented by a ball-and-sticks model and first-shell water molecules are drawn as cylinders and linked to the central ion by green dashed lines. Selected H-bonds are shown as blue arrows. Structural changes of the ligand coordination sphere are displayed as yellow arrows.

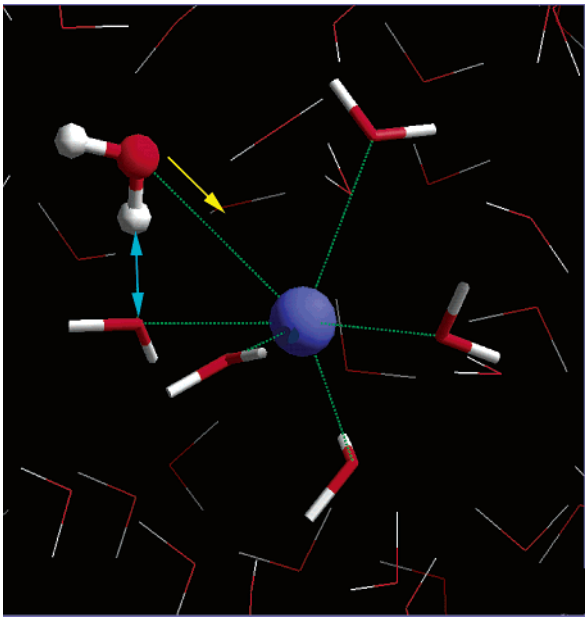

Figure 9. Transition state geometry of reaction 1 for the sodium ion. The incoming water (WAT) is represented by a ball-and-sticks model and first-shell water molecules are drawn as cylinders and linked to the central ion by green dashed lines. Selected H-bonds are shown as blue arrows. Structural changes of the ligand coordination sphere are displayed as yellow arrows.

The exchange reaction turns out to occur mostly via a substitution mechanism (Figure 8). However, also addition and elimination processes are observed.

At the transition state of the substitution mechanism the oxygen belonging to the approaching water interacts with both the metal ion and a water molecule belonging to the second shell (Figure 8 and Table 2). Its presence induces a distortion in the potassium coordination polyhedron, accompanied by a weakening of the interaction between the metal ion and one of the water binding to it. The latter eventually leaves the K^+ coordination sphere assisted by the formation of a hydrogen bond with another metal-bound water. In the absence of the formation of this last hydrogen bond, addition of the approaching water to the ion is observed. Our MSMD simulations provide the same mechanistic picture for the addition mechanism.

The calculated free energy of the process has a plateau in the bulk region followed by a maximum at 3.4 corresponding to the activated complex, and a minimum at about 2.7 Å (Table 2). The latter value represents the optimal ion−water distance and is in agreement with the maximum of the radial pair distribution function (Table 1, and Figures 1 and 7).

Sodium. In our equilibrium simulations Na^+ is coordinated by five and, more often (66% of the time), by six water molecules (average coordination number $n = 5.7$). The penta- and hexacoordinated complexes are stable for more than 10 ps and exhibit clear trigonal bipyramidal and octahedral equilibrium geometries.

The water exchange mechanism occurs via an associative/dissociative pathway, in which the sodium coordination number changes from 5 to 6 and vice versa. In the associative process, the approaching water molecule forms a hydrogen bond to one of the water molecules bound to the metal ion; subsequently, it enters the coordination sphere. The transition state (Figure 9 and Table 2) is a distorted octahedral structure, in which the incoming water still forms an H-bond to a metal-bound water molecule (Figure 9 and Table 2). Finally, the geometry of the coordination polyhedron relaxes to an octahedral structure.

In the dissociative process, the 6-coordinated complex undergoes relatively large structural fluctuations, which at times cause the formation of an H-bond between two metal-bound water molecules. This induces the release of one of the water ligands and reformation of the trigonal-bipyramidal geometry. Thus, basically, the mechanism of the associative part of the reaction is the direct inverse of its dissociative counterpart.

These mechanisms have also been observed in a recent ab initio molecular dynamics simulation.[40] Furthermore, the characteristic time scale of the process (about 0.3 ps) is also similar to that of the ab initio calculation.[40]

In our MSMD simulations, reaction 1 occurs via the same mechanisms observed for the unconstrained ones. The free energy profile of the process is plotted in Figure 6. As expected, the free energy barrier is larger and the minimum less pronounced than the corresponding values for potassium. As in the case of K^+, the energy minimum corresponds essentially to the maximum of the $g_{MO_w}(r)$ $R_0 = 2.43$ Å (see Figures 1−7 and Tables 1−2).

5. Conclusions

Our calculations provide an energetic and structural description of water exchange at alkali ions in aqueous solution using the MSMD approach.[1,2,7,8]

The convergence of the free energy profiles depends on the steering velocity and on the initial sampling conditions. A proper choice of these key parameters leads to fast convergence by averaging only a limited number of simulations (≤ 10).

As expected, the solvation shell of sodium and, even more so, the one of potassium are highly flexible. It includes dynamical structures involving varying numbers of coordinated water molecules and different geometries within each coordination number. The water exchange reaction (eq 1) for potassium occurs with a direct substitution mechanism.

In contrast, for sodium, it takes places via an associative/dissociative mechanism, in which the coordination of the metal goes from trigonal bipyramid to octahedral and vice versa. Both

processes are assisted by the formation and breaking of H-bonds between the incoming water molecule and the metal ligands. These results are in good agreement with recent ab initio calculations.[40]

In conclusion, the MSMD technique appears to be a very powerful, fast, and reliable technique to study chemical processes. This approach holds great promise for free energy evaluations in complex systems with relatively long relaxation times, where molecular dynamics simulations cannot lead to the direct observation of the physically interesting events. Particularly attractive is the use of this approach in combination with ab initio molecular dynamics techniques, which is expected to provide a relatively fast route to the calculations of free energy activation barriers of chemical and enzymatic reactions.[41]

Acknowledgment. This work is supported by INFM and MURST cofin. We thank Prof. Jarzynski for useful discussions.

References and Notes

(1) Jarzynski, C. *Phys. Rev. Lett.* **1997**, *78*, 2690−2693.
(2) Jarzynski, C. *Phys. Rev. E* **1997**, *56*, 5018−5035.
(3) Hille, B. *Ionic Channels of Excitable Membranes*; Sinauer Associates: 1992.
(4) Guidoni, L.; Torre, V.; Carloni, P. *Biochemistry* **1999**, *38*, 8599−8604.
(5) Zhou, Y.; Morais-Cabral, J. H.; Kaufman, A.; McKinnon, R. *Nature* **2001**, *414*, 43−49.
(6) Helm, L.; Merbach, A. E. *Coord. Chem. Rev.* **1999**, *187*, 151−181.
(7) Crooks, G. E. *Phys. Rev. E* **2000**, *61*, 2361−2366.
(8) Hummer, G.; Szabo, A. *Proc. Natl. Acad. Sci. U.S.A.* **2001**, *98*, 3658−3661.
(9) Grubmüller, H.; Heymann, B.; Tavan, P. *Science* **1996**, *271*, 997−999.
(10) See, e.g.: (a) Balsera, M.; Stepaniants, S.; Izrailev, S.; Oono, Y.; Schulten, K. *Biophys. J.* **1997**, *73*, 1281−1287. (b) Marszalek, P. E.; Lu, H.; Li, H.; Carrion-Vazquez, M.; Oberhauser, A. F.; Schulten, K.; Fernandez, J. M. *Nature* **1999**, *402*, 100−103.
(11) Perkins, T. T.; Smith, D. E.; Chu, S. *Science* **1994**, *264*, 819−822.
(12) Florin, E. L.; Moy, V. T.; Gaub, H. E. *Science* **1994**, *264*, 415−417.
(13) Strick, T. R.; Allemand, J. F.; Bensimon, D.; Bensimon, A.; Croquette, V. *Science* **1996**, *271*, 1835−1837.
(14) Smith, S. B.; Cui, Y. J.; Bustamante, C. *Science* **1996**, *271*, 795−799.
(15) Tskhovrebova, L.; Trinick, J.; Sleep, J. A.; Simmons, R. M. *Nature (London)* **1997**, *387*, 308−312.
(16) Rief, M.; Gautel, M.; Oesterhelt, F.; Fernandez, J. M.; Gaub, H. E. *Science* **1997**, *276*, 1109−1112.
(17) Oberhauser, A. F.; Marszalek, P. E.; Erickson, H. P.; Fernandez, J. M. *Nature (London)* **1998**, *393*, 181−185.
(18) Oesterhelt, F.; Oesterhelt, D.; Pfeiffer, M.; Engel, A.; Gaub, H. E.; Müller, D. J. *Science* **2000**, *288*, 143−146.
(19) Merkel, R.; Nassoy, P.; Leung, A.; Ritchie, K.; Evans, E. *Nature (London)* **1999**, *397*, 50−53.
(20) Kellermayer, M. S. Z.; Smith, S. B.; Granzier, H. L.; Bustamante, C. *Science* **1997**, *276*, 1112−1116.
(21) Isralewitz, B.; Izrailev, S.; Schulten, K. *Biophys. J.* **1997**, *73*, 2972−2979.
(22) Marszalek, P. E.; Lu, H.; Li, H.; Carrion-Vazquez, M.; Oberhauser, A. F.; Schulten, K.; Fernandez, J. M. *Nature (London)* **1999**, *402*, 100−103.
(23) Paci, E.; Karplus, M. *J. Mol. Biol.* **1999**, *288*, 441−459.
(24) Hendrix, D. A.; Jarzynski, C. *J. Chem. Phys.* **2001**, *114*, 5974−4981.
(25) Hummer, G. *J. Chem. Phys.* **2001**, *114*, 7330−7337.
(26) Jensen, M. Ø.; Park, S.; Tajkhorshid, E.; Schulten, K. *Proc. Natl. Acad. Sci. U.S.A.* **2002**, *99*, 6731−6736.
(27) Case, D. A.; Pearlman, D. A.; Caldwell, J. W.; Cheatham, T. E., III; Ross, W. S.; Simmerling, C. L.; Darden, T. A.; Merz, K. M.; Stanton, R. V.; Cheng, A. L.; Vincent, J. J.; Crowley, M.; Ferguson, D. M.; Radmer, R. J.; Seibel, G. L.; Singh, U. C.; Weiner, P. K.; Kollman, P. A. *AMBER*, version 5, University of California: San Francisco, 1997.
(28) Åqvist, J. *J. Phys. Chem.* **1990**, *94*, 8021−8024.
(29) Smith, D. E.; Dang L. X. *J. Chem. Phys.* **1994**, *100* (5), 3757−3766.
(30) Jorgensen, W. L. *J. Chem. Phys.* **1983**, *79* (2), 926−935.
(31) Darden, T.; York, D.; Pedersen, L. G. *J. Chem. Phys.* **1993**, *98*, 10089−10092.
(32) Essman, U.; Perera, L.; Berkowitz, M. L.; Darden, T.; Lee, H.; Pedersen L. G. *J. Chem. Phys.* **1995**, *103*, 8577−8593.
(33) Berendsen, H. J. C.; Postma, J. P.; Di Nola, A.; Van Gunsteren, W. F.; Haak, J. R. *J. Chem. Phys.* **1984**, *81*, 3684−3690.
(34) Ramaniah, L. M.; Bernasconi, M.; Parrinello, M. *J. Chem. Phys.* **1999**, *111*, 1587−1591.
(35) Lee, S. H.; Rasaiah, J. C. *J. Chem. Phys.* **1994**, *101*, 6964−6974.
(36) Obst, S.; Bradaczek, H. *J. Phys. Chem.* **1996**, *100*, 15677−15687.
(37) Impey, R. W.; Madden, P. A.; MacDonald, I. R. *J. Phys. Chem.* **1983**, *87*, 5071.
(38) Skipper, N. T.; Neilson, G. W. *Chem. Phys. Lett.* **1985**, *114*, 35.
(39) Skipper, N. T.; Neilson, G. W. *J. Phys.: Condens. Matter* **1989**, *1*, 4141.
(40) White, J. A.; Schwegler, E.; Galli, G.; Gygi, F. *J. Chem. Phys.* **2000**, *113*, 4668−4673.
(41) Carloni, P.; Rothlisberger, U.; Parrinello, M. *Acc. Chem. Res.* **2002**, *35*, 455−464.